inorganics

MDPI

Article

Stabilization of Supramolecular Networks of Polyiodides with Protonated Small Tetra-azacyclophanes

Matteo Savastano [1,*], Álvaro Martínez-Camarena [2], Carla Bazzicalupi [1], Estefanía Delgado-Pinar [2], José M. Llinares [2,3], Palma Mariani [1], Begoña Verdejo [2], Enrique García-España [2,*] and Antonio Bianchi [1]

1 Department of Chemistry "Ugo Schiff", University of Florence, Via della Lastruccia 3, 50019 Sesto Fiorentino, Italy; carla.bazzicalupi@unifi.it (C.B.); palma.mariani@unifi.it (P.M.); antonio.bianchi@unifi.it (A.B.)

2 ICMol, Department of Inorganic Chemistry, University of Valencia, C/Catedrático José Beltrán 2, 46980 Paterna, Spain; alvaro.martinez@uv.es (Á.M.-C.); estefania.delgado@uv.es (E.D.-P.); jollibe@uv.es (J.M.L.); begona.verdejo@uv.es (B.V.)

3 Departamento de Química Orgánica, Universidad de Valencia, C/Dr. Moliner s/n, 46100 Burjassot, Valencia, Spain

* Correspondence: matteo.savastano@unifi.it (M.S.); enrique.garcia-es@uv.es (E.G.-E.)

Received: 1 March 2019; Accepted: 26 March 2019; Published: 1 April 2019

Abstract: Polyiodide chemistry is among the first historically reported examples of supramolecular forces at work. To date, owing to the increasingly recognized role of halogen bonding and the incorporation of iodine-based components in several devices, it remains an active field of theoretical and applied research. Herein we re-examine azacyclophanes as a class of ligands for the stabilization of iodine-dense three-dimensional networks, showing how we devised novel possible strategies starting from literature material. The new set of azacyclophane ligands affords novel crystal structures possessing intriguing properties, which develop on a double layer. At a macroscopic level, the obtained networks possess a very high iodine packing density (less than 2 times more diluted than crystalline I_2): a simple parameter, I_N, is also introduced to quickly measure and compare iodine packing density in different crystals. On the microscopic level, the present study provides evidence about the ability of one of the ligands to act as a three-dimensional supramolecular mold for the template synthesis of the rarely observed heptaiodide (I_7^-) anion. Therefore, we believe our approach and strategy might be relevant for crystal engineering purposes.

Keywords: iodine; polyiodides; azacyclophanes; heptaiodide; supramolecular forces; iodine networks; anion coordination chemistry

1. Introduction

The earliest observations of some of the most recently recognized intermolecular forces, like halogen–halogen interactions, trace back to Gay Lussac's pioneering assertions about the ability of iodide to weakly retain molecular iodine [1,2]. To date, supramolecular chemistry of polyiodide systems remains a challenging and interesting topic, as these species generally manifest both a hypervalent behavior and a marked ability to catenate between themselves through intermolecular donor–acceptor interactions, which are heavily dependent onto their local chemical environment and on the nature of counterions [3]. Such features are gradually coming into the spotlight the more we become able to recognize and understand halogen bonding in these systems and direct polyiodide assembly [3–11]. Moreover, polyiodide systems have recently encountered a broad technological interest, mainly connected with solar energy harvesting and storage, e.g., dye-sensitized solar cells

and batteries, where they have been successfully implemented as electrolyte in various forms [12,13]. Solid-state conductors based on the Grotthus conduction mechanism [3,14] are also a major field of research [15–17]; on this side some of us recently reported about the possibility of using supramolecular forces, such as the strong anion–π interactions exerted by s-tetrazines [18], to direct the assembly of polyiodide networks [19].

Azacyclophanes have long been in the spotlight as pH-dependent anion receptors [20]. Moreover, some interesting results concerning the ability of these ligands to stabilize polyiodides, including the elusive I_4^{2-} anion, when in their protonated form [21], prompted us to investigate further concerning their binding possibilities. According to Ilioudis and Steed, stabilization of such species were made possible by the good structural complementarity of the rather large 3,10,17-Triazabicyclo[17.3.1]tricosa-1(23),19,21-triene with the iodide anion, which proved effective in stabilizing highly charged species such as I_4^{2-}. However, hydrogen bonding was not found to be a prominent force and the organization of less charge dense (I_8^{2-}) polyiodide network was also observed around the ligand.

In this work, instead, we discuss the use of small protonated azacyclophanes for the stabilization of polyiodide networks. Size mismatch between the two interacting partners and nesting of the charged ammonium sites deep within the azacyclophane cage appealed to us as a way to foster the formation of large hydrophobic iodine-rich cages surrounding relatively small ligands, actively promoting the formation of iodine-dense packings.

The experimental design followed in the present work was mainly guided by two literature sources, the results of which deserve a quick analysis here for the purpose of contrasting and comparing them with our findings.

The main literature source, as anticipated above, is ref [21]. The ligand proposed by Ilioudis and Steed (Figure 1a) presents an almost perfect size/shape complementarity to the iodide anion ([21] and Figure 1b,c), resulting in its effective coordination by the ligand. It is worth noticing that, arguably due to said complementarity, charged iodine species (namely the tip of I_4^{2-} ion or iodide ion, Figure 1b,c) are always found interacting with the macrocycle. Neutral iodine molecules and/or less charge-dense higher polyiodide species (I_8^{2-}) preferentially interact with the hydrophobic hydrocarbon backbone of the ligand instead (Figure 1d).

Other helpful insights were drawn from the structure of the hydrobromic salt of 3,6,9-triaza-1(2,6)-pyridinecyclodecaphane (L1) which became the starting point of current work [22]. As can be seen from Figure 2, the marked basicity of the ligand [22–24] (the extra aza-type nitrogen helping to compensate for the loss of basicity due to the proximity of charged groups compared to the azacyclophane used in [21]) pairs with its small size, so that even in the case of the significantly smaller (compared to I^-) bromide, only one anion can be accommodated above the macrocycle; yet it may not engage all N atoms into salt-bridge/hydrogen bonding (Figure 2a,b). Specifically, triprotonated L1 is observed to only manage to use proximal aliphatic ammonium groups as convergent binding sites (Figure 2a) (proximal N···N distance 3.079(3) Å), but not the two distal ones (i.e., those separated by the pyridine ring) (distal N···N distance 5.471(3) Å). To accommodate all the necessary counterions, the ligand is forced to use its ammonium groups as divergent binding sites, so that further bromide anions can be trapped within three-dimensional cavities formed in between the ligand molecules (Figure 2c). This was considered as an indication of the ability of this ligand to force the localization of charged species outside its cage and stabilize them in three-dimensional supramolecular networks.

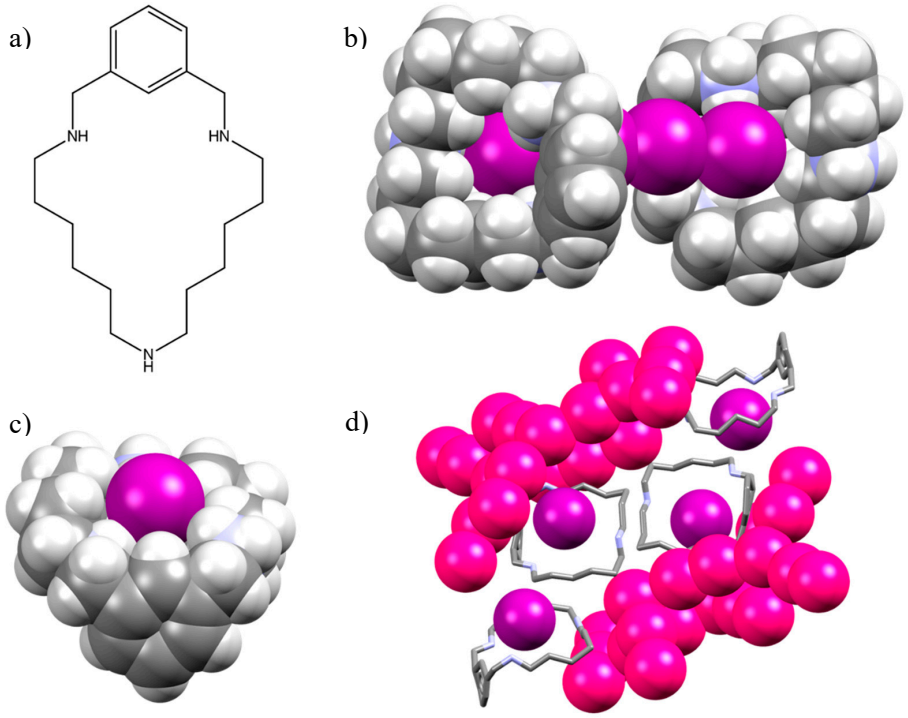

Figure 1. Summary of the crystallographic results presented in [21] as functional to the current discussion. Color code: white, H; grey, C; cyan, N; violet, I; I_8^{2-} networks highlighted in pink. (**a**) Structure of the large azacyclophane triazabicyclo[17.3.1]tricosa-1(23),19,21-triene employed as a ligand. Evidence of ligand-iodide size/shape complementarity: (**b**) as found in the I_4^{2-} complex (CSD refcode NABWOD [21]) and (**c**) in the mixed iodide–I_8^{2-} complex (CSD refcode NABWUJ [21]); (**d**) I_8^{2-} network (in pink) (CSD refcode NABWUJ [21]) mainly developing around the external hydrophobic rim of the cyclophane.

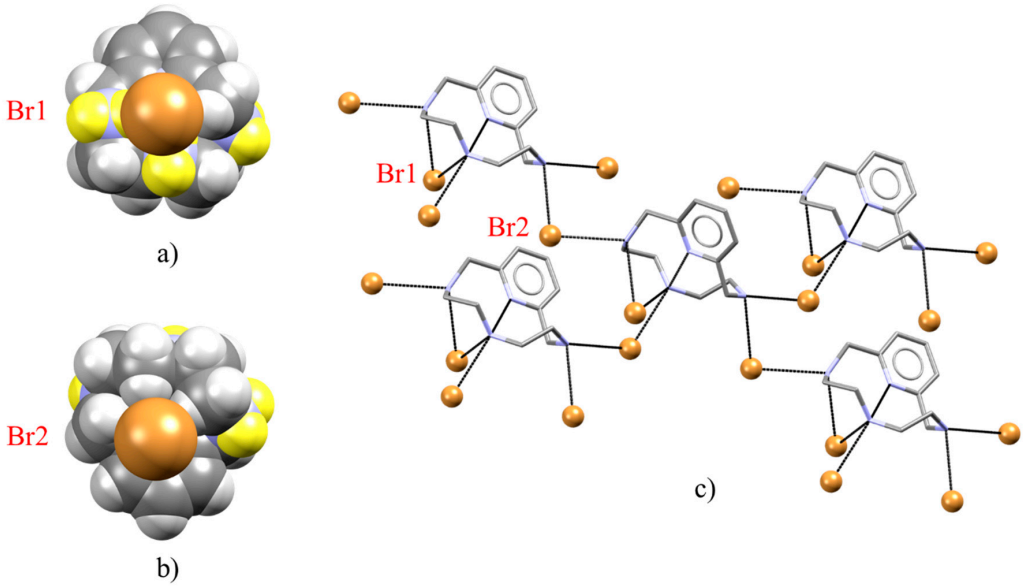

Figure 2. Summary of the crystallographic results presented in [22] (CSD refcode SIBHOC) as functional to current discussion. Color code: white, H; grey, C; cyan, N; brown, Br; H belonging to ammonium groups are highlighted in yellow. (**a**) Detail of the H_3L1^{3+}–Br1 interaction showing the ligand steric impossibility to bring all its ammonium groups towards the anion; (**b**) the other face of H_3L1^{3+} interacting only via C–H anion contacts with Br2; (**c**) the 3-dimensional hydrogen bond network (in black) as found in the $[H_3L1(Br)_3]$ salt.

In the case of iodine-based species the hydrogen bonding contribution was expected, and found [21] to be more modest than for bromide, while hydrophobic contacts are expected to play a major role in stabilizing scarcely charged polyiodides. Accordingly, we adopted methylation as a tool to gradually modify the ligands, eventually forcing the hydrogen bond network nesting inside the cyclophane structure, leaving a hydrophobic external surface suitable for iodine interaction. The ligands employed in this work are reported in Figure 3.

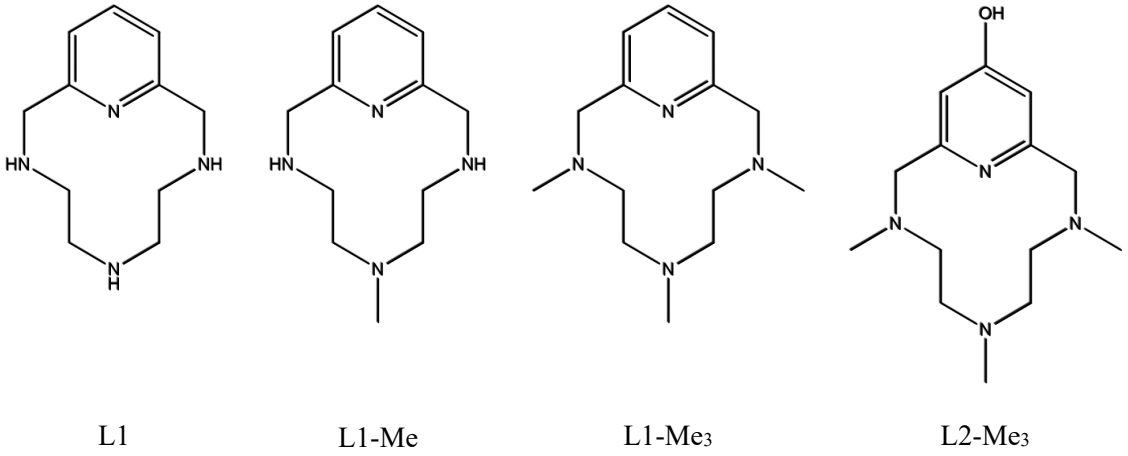

L1 L1-Me $L1\text{-}Me_3$ $L2\text{-}Me_3$

Figure 3. Structural formulas of the ligands employed in the current study.

Regrettably, despite considerable efforts, only protonated forms of L1 and L2–Me_3 furnished single crystals of polyiodide complexes suitable for X-ray diffraction (XRD) studies. Nevertheless, the obtained crystalline samples present some fascinating structural features.

2. Results

2.1. Crystal Structure of $[(H_2L1)_2I_2(I_5)(I_3)_3]$

This structure consists of diprotonated L1 ligands, polyiodide anions and iodine molecules. The asymmetric unit contains two non-equivalent ligands, one I_5^-, three I_3^- anions and two halves of non-equivalent I_2 molecules (Figure 4).

Each ligand assumes a bent conformation featuring 148° and 145° dihedral angles between the aromatic ring plane and the mean plane defined by the aliphatic nitrogen atoms, respectively. All the aliphatic nitrogen atoms interact via H-bonds with the polyiodide anion (Table S1). Most of these contacts are rather long (minimum 3.566 Å, maximum 3.922 Å, and average 3.7 ± 0.1 Å) and it is worth noticing how they rarely (with the exception of I9) involve the central, formally charge-bearing atoms of polyiodides (even considering a $I_3^-{\cdot}I_2$ description for the pentaiodide anion, see below). This indicates either that classic charge–charge interactions have little influence in orchestrating the overall packing or that valence in the polyiodide network goes beyond what can be predicted on a qualitative level, or both. Relevant information on this point is provided by the iodine molecules (Figure 5). Beyond being stabilized by CH···I interactions from neighboring ligand molecules, both I_2 molecules are sandwiched between I_3^- (I16–I16′) or I_5^- (I13–I13′) anions (Figure 5). Close inspection reveals I–I distances in the iodine molecules of 2.812(1) Å (I13–I13′) and 2.816(2) Å (I16–I16′), i.e., longer than those of molecular iodine (2.715 Å) [3], while also the interacting polyiodide anions are found asymmetric (I_3^-: I6–I2 2.8188(8) Å, I2–I5 3.0707(8) Å; I_5^-: I4–I1 2.9234(7) Å, I1–I3 2.8905(7) Å, I10–I12 2.7723(8) Å, I3–I12 3.2541(8) Å). This creates a succession of alternating long–short inter- and intramolecular distances, displayed in Figure 5, which is typical of iodine–iodine secondary bonds. This term, introduced in its general usage by Alcock [25], is employed in polyiodide chemistry to describe I···I intermolecular interactions in the 3.4–3.7 Å range [3], i.e., supramolecular interactions which nevertheless involve a certain degree of orbital interaction. Accordingly, the formation of secondary

bonds is always accompanied by a weakening of intramolecular bonds of the involved polyiodide species. The alternating long-short inter and intra molecular distances of Figure 5 clearly indicate orbital interactions between polyiodides (I_3^-, I_5^-) and I_2 molecules (Figure 5), so that, as strong secondary bonds are formed, covalent interactions are loosened.

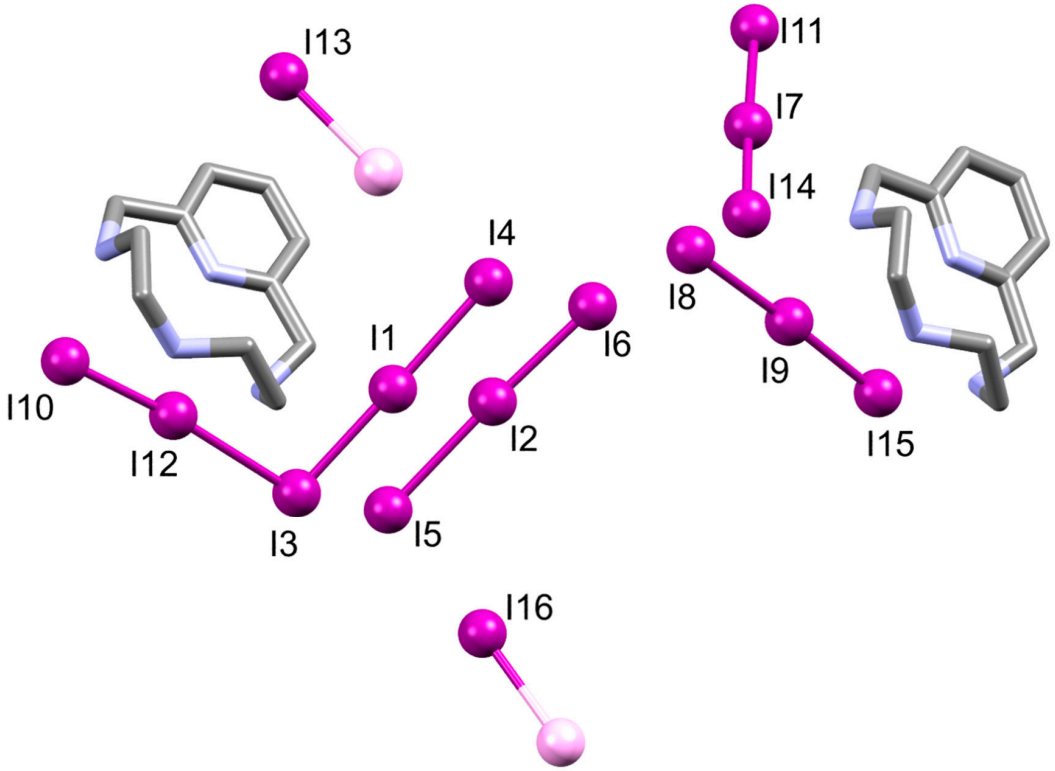

Figure 4. Content of the asymmetric unit of the $[(H_2L1)_2I_2(I_5)(I_3)_3]$ crystals. Color code: white, H; grey, C; cyan, N; violet, I; halved non-equivalent I_2 molecules have been completed in the picture in light violet to avoid misperception.

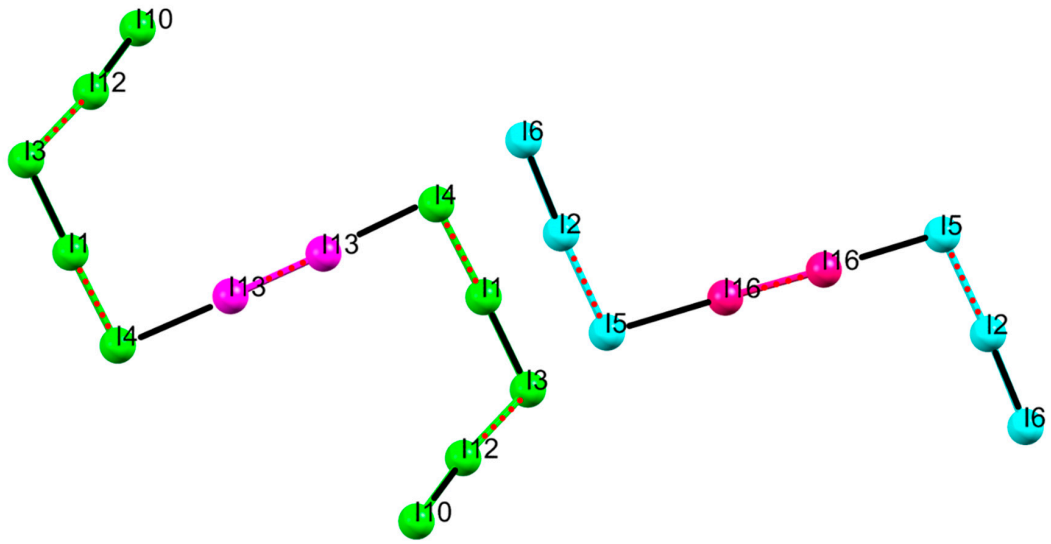

Figure 5. Detail of the long-short alternating I–I interatomic distances involving the two I_2 molecules found within the crystal structures. Inter- and intramolecular interatomic distances which are found shorter than reference values are displayed with solid black lines, those which are found longer are displayed with dotted red lines. Arbitrary color is used to mark symmetry equivalent polyiodides.

The high asymmetry observed for the pentaiodide anion suggests this species is better rationalized, as often observed in the literature, [3] as a I_3^- anion (I3–I1–I4) strongly interacting with an iodine molecule (I12–I10). As a matter of fact, this disguised iodine molecule is also sandwiched between the strongly interacting (I3–I1–I4) triiodide and the I11–I7–I14 triiodide, which in turn is also interacting with the last triiodide (I15–I9–I8) found in the crystal structure. As a consequence of the network formed by secondary bonds, all I_3^- anions in the crystal structure are found asymmetric (I11–I7 3.1083(8) Å, I7–I14 2.7866(9) Å; I8–I9 3.0523(8) Å, I9–I15 2.8172(8) Å; I6–I2 2.8188(8) Å, I2–I5 3.0707(8) Å).

The result of these significant iodine–iodine secondary bonds is a polyiodide network constituted of zig-zag chains involving all the iodine-based species in the crystals. These chains leave void open channels where the protonated ligands are hosted, to the point that the whole structure appears as a sort of self-assembled supramolecular clathrate (Figure 6).

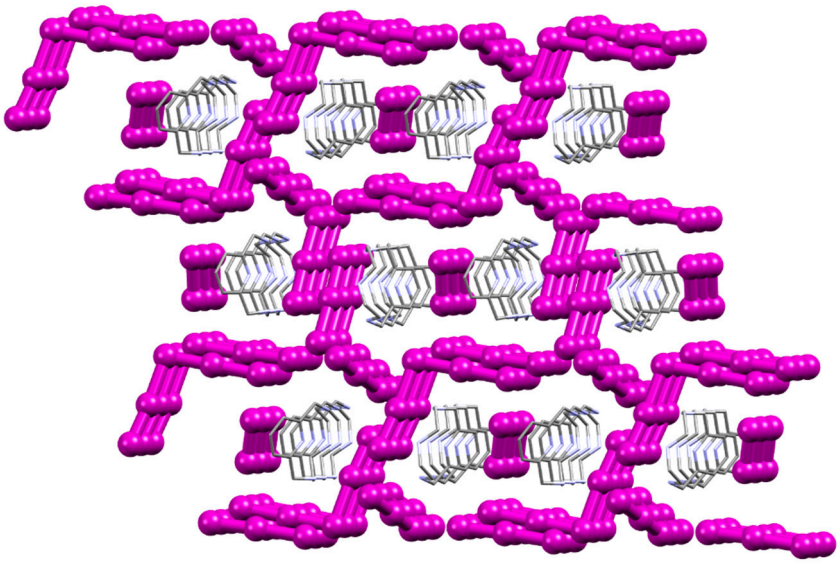

Figure 6. View of the lattice formed by polyiodides and iodine molecules resulting in a self-assembled clathrate structure trapping the H_2L1^{2+} counterions in its cavities. Color code: grey, C; cyan, N; violet, I.

2.2. Crystal Structure of [H_2L2-Me_3(I_7)$_2$]

The structure consists of diprotonated L2–Me_3 ligands and I_7^- anions, each lying on the crystallographic planes (Figure 7). The ligand assumes a bent conformation, typical of small macrocycles incorporating rigid aromatic units [22–24,26,27], which can be described by the 84° dihedral angle between the aromatic ring plane and the mean plane defined by the aliphatic nitrogen atoms. The acidic protons are located on the benzylic nitrogen atoms [22–24], yet their interaction with the polyiodide anions are very limited, consisting of a sole contact, and moreover quite long to be considered a typical salt bridge (N2(H2A)···I6 3.753 Å). The same can be said for the OH group, giving an additional long H···I contact (O1(H1)···I5 3.779 Å). Each I_7^- anion assumes a pyramidal conformation with bond angles at the apical iodine atom of 84°, 84° and 93° (A Figure 7) and 83°, 83° and 102° (B Figure 7). The I–I terminal bond distances are in the range 2.75(1)–2.815(3) Å while the I–I distances from the apical iodine vary from 3.061(3) to 3.233(2) Å. The overall symmetry (angles and distances) of the heptaiodides is higher than those observed for reported I_7 (cf. Discussion section), however, this aspect cannot be discussed meaningfully because such symmetry originates from the fact that the anions lay on crystallographic planes. Both the terminal and the apical iodine atoms are involved in short I···I intermolecular contacts which can be considered as secondary bonds (I3···I10 3.46(1) Å) or van der Waals interactions (below 4 Å): as can be seen in Figure 8, the central iodine atom of B, formally bearing the charge, forms the strongest interaction with neighboring I_7^- A anions linearly along I–I covalent bonds, i.e., respecting the typical geometry expected from σ-hole

interactions. As in the case of the $[(H_2L1)_2I_2(I_5)(I_3)_3]$ crystals, the whole crystal structure can be defined as a iodine-based clathrate structure trapping the diprotonated $H_2L2–Me_3^{2+}$ ligand molecules, but in this case the formed architecture is even more striking: as shown in Figure 9 the contacts between I_7^- anions define a slightly distorted void cubic lattice hosting the countercations. A global view of the packing is reported in Figure 10.

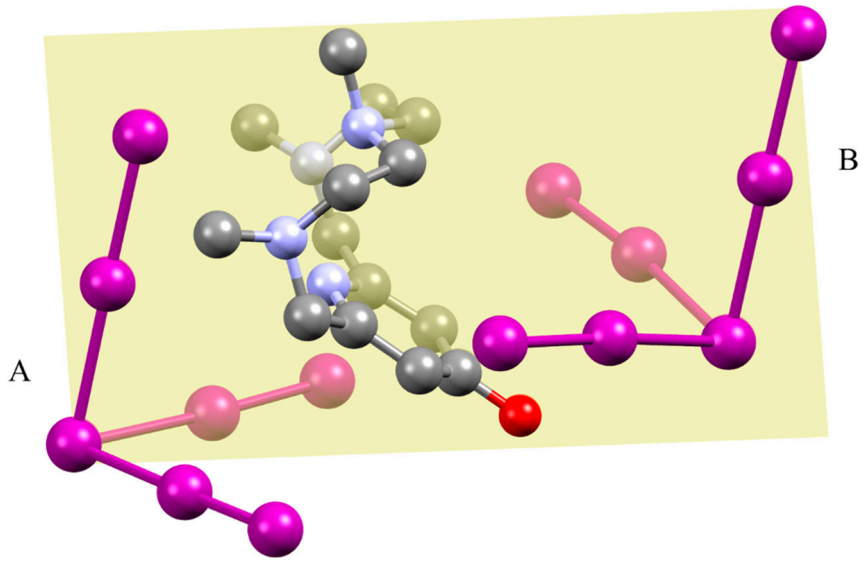

Figure 7. Depiction of the asymmetric unit of the $[H_2L2–Me_3(I_7)_2]$ crystals. All ions are halved by a crystallographic plane (in yellow) and have been here completed for simplicity. Non-equivalent heptaiodide anions are marked as A or B for reference. Color code: grey, C; cyan, N; red, O; violet, I.

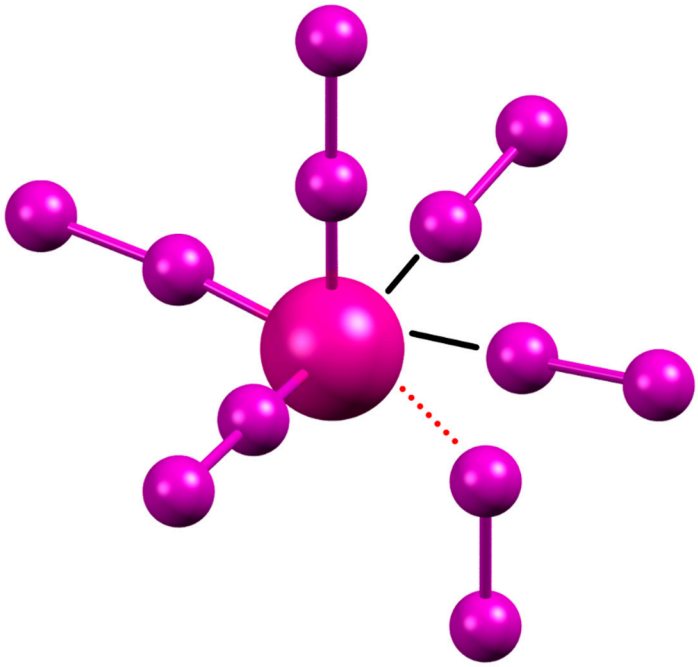

Figure 8. I···I contacts found among the central atom of I_7^- B (highlighted in purple) and neighboring heptaiodides. Short secondary bonds are found linear according to σ-hole type interactions (black solid lines), longer contacts do not respect such geometry (red dotted line).

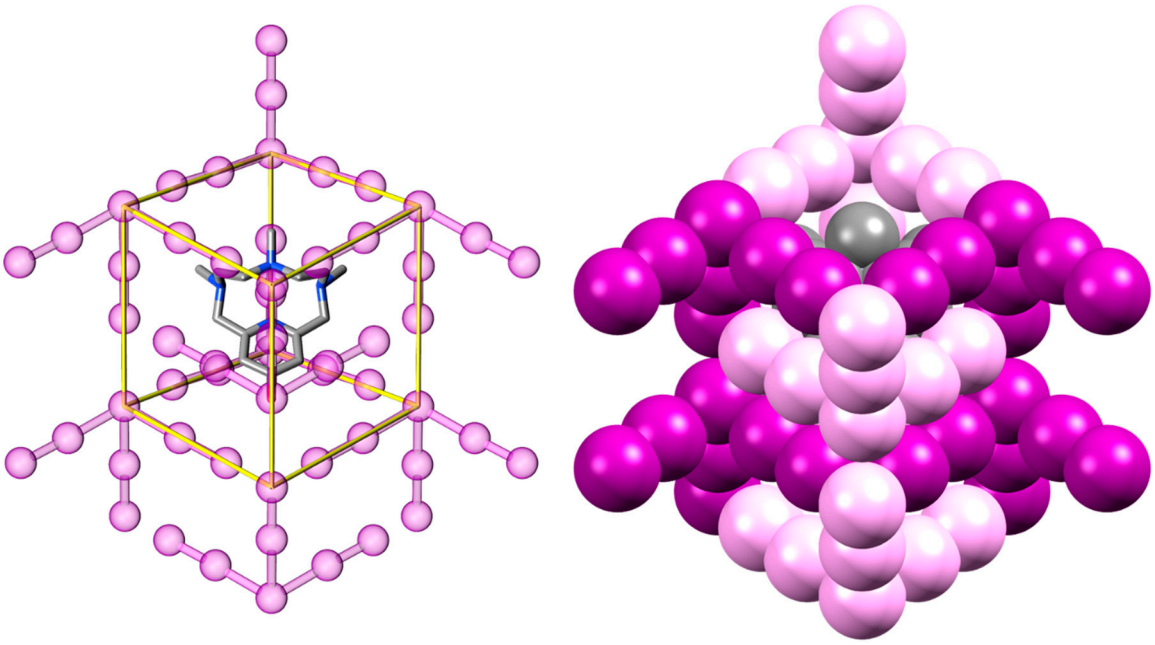

Figure 9. Schematic depiction of the distorted cubic lattice (yellow) formed by heptaiodide anions around the $H_2L–Me_3^{2+}$ counterions (left) and space filling version of the same view showing the total encapsulation of the ligand (right). Color code: grey, C; cyan, N; red, O; violet, I; different shades of violet are used to help identifying discrete I_7^- ions.

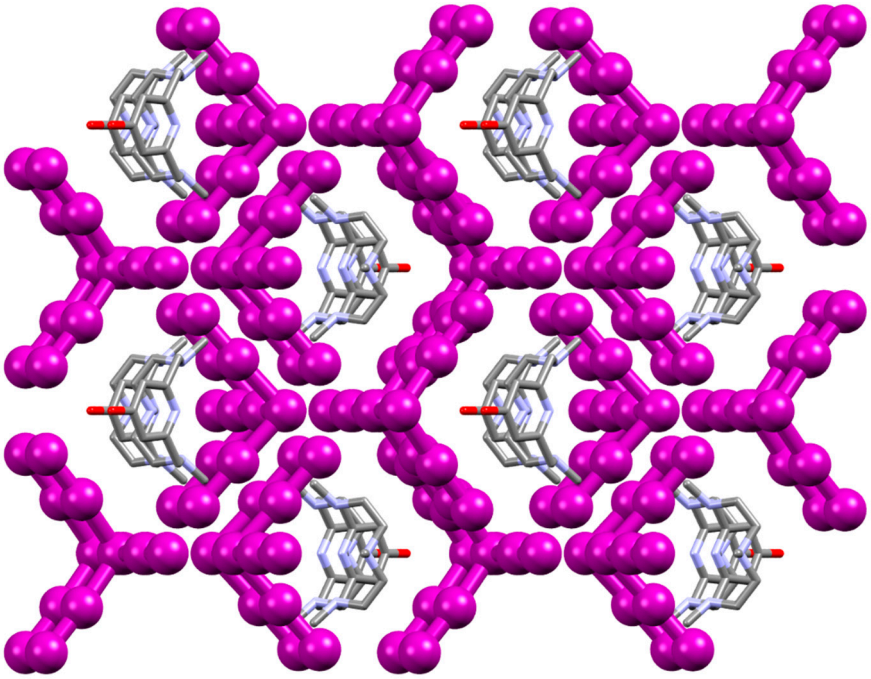

Figure 10. Global view of the packing found in the $[H_2L2–Me_3(I_7)_2]$ crystal. Color code: grey, C; cyan, N; red, O; violet, I.

3. Discussion

Analysis and comparison with literature data of the obtained structures can be undertaken both at a macroscopic and a microscopic level.

On a macroscopic level, density of iodine is an important parameter for possible practical applications, especially as solid-state conductors. This is because, as logical and reported [3], chance

of short I···I distances allowing for orbital interactions and electron conduction via a Grotthus-like mechanism [3,14], increases the more the iodine atoms are densely packed.

We propose as an easy macroscopic descriptor, allowing for direct comparison between different crystal structures, a quantity I_N, or Iodine Number. This is easily calculated. Counting the I atoms found within a unit cell and dividing for the cell volume gives the crystal average iodine number density per Å^3, a rather inconvenient parameter to utilize as it is (we get to know that very small decimal fractions of I atoms can be included in a volume as small as 1 Å^3). The I_N is defined as the ratio of the iodine number density per Å^3 of the crystal under examination to the iodine number density per Å^3 of crystalline molecular iodine (reference state in standard conditions).

Iodine number density in I_2 crystals has a value of 0.02346 Å^{-3}. It is instructive to show the qualitative meaning of such a number. An isolated I atom treated as a hard sphere of radius 2.04 Å [28], i.e., occupying 35.6 Å^3, would have an I number density of 0.02812 Å^{-3}. Dense packing of spheres has a packing efficiency of ≈0.74, meaning that the maximum theoretical I number density under hard spheres packing approximation would be 0.02079 Å^{-3}. Crystalline molecular iodine possesses an even higher I number density than that (0.02346 Å^{-3}, i.e., it is roughly 12% more dense than the theoretical hard spheres packing): this is due to the molecular nature of I_2, which allows spheres to interpenetrate significantly. According to its high packing density and significance, we decided to use I number density of crystalline I_2 as a reference limit value for comparing iodine packing densities within different crystals: by definition of I_N, crystalline molecular I_2 has an $I_N = 1$.

When we move from the I_4^{2-} complex of NABWOD (Figure 1b) [21] ($I_N = 0.285$), to the I_8^{2-} network in NABWUJ (Figure 1d) [21] ($I_N = 0.420$), then to the crystal structure of $[(H_2L1)_2I_2(I_5)(I_3)_3]$ ($I_N = 0.527$) and finally to the heptaiodide complex $[H_2L2–Me_3(I_7)_2]$ ($I_N = 0.589$), I_N numerical values are effective in immediately suggesting how much denser the iodine packing gradually becomes (from 3.5 times more diluted than the reference, NABWOD, to less than two times more diluted than reference, $[H_2L2–Me_3(I_7)_2]$). This reflect itself in the gradual shift from isolated I_4^{2-} ions bound by cyclophanes (Figure 1b) [21], to three-dimensional ribbons of polyiodides interacting with the ligands (Figure 1d) [21], to polyiodide structures forming channels hosting small azacyclophanes (Figure 6), up to clathrate-like cages completely engulfing the ligand (Figure 10).

According to these observations it is safe to conclude that the choice of small azacyclophanes actively promotes a dense packing of the polyiodide anions, rather than the coordination of discrete anions observed with a cyclophane matching the size of the iodide anion [21].

The microscopic description level has a twofold importance. On the applicative side, having an iodine packing which is dense on average (e.g., as view from a macroscopic descriptor like I_N), does not necessarily imply that an uninterrupted I···I secondary bond network capable of functioning as an electron conductor exists within the crystal. This is the reason we dedicated much of the crystallographic section to the description of the I···I intermolecular contacts. On a theoretical side, which is more of concern at present, evaluation of forces in play through the observed contacts are paramount for the understanding of these packings and the recognition of novel crystal engineering strategies.

As anticipated from the beginning, indeed the nesting of the hydrogen bond network within the frame of small azacyclophanes resulted in a lesser dependence of the packing on salt bridge interactions. This can be easily observed from the comparison of Figure 11 with Figures 1 and 2.

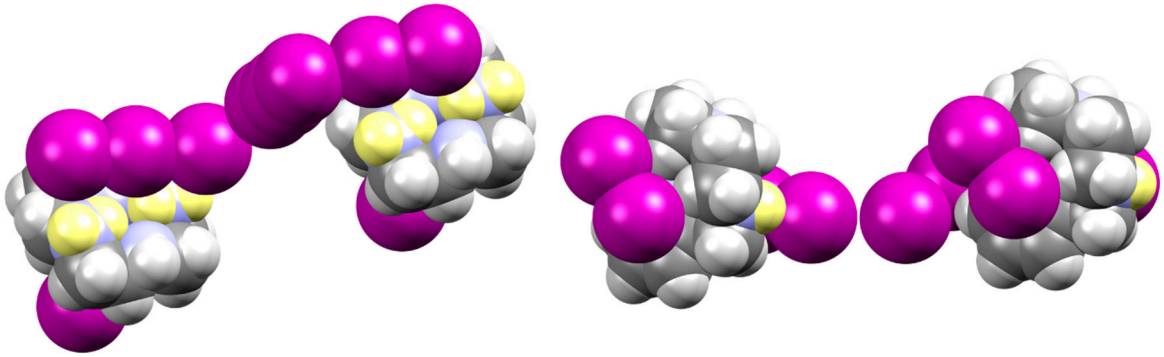

Figure 11. View of both sides of the azacyclophanes and of their interactions with iodine-based species as found in the $[(H_2L1)_2I_2(I_5)(I_3)_3]$ crystal structure. Color code: white, H; grey, C; cyan, N; violet I; H belonging to ammonium groups are highlighted in yellow.

As can be seen, the hydrophilic face of the azacyclophanes presenting the ammonium groups is found interacting either with a triiodide or with the iodine molecule strongly bound to a triiodide within the pentaiodide anion. Neither convergence of ammonium groups towards a specific anionic site, nor the encapsulation induced by the perfect fit observed in Figure 1 are possible here. Conversely, the hydrophobic face of the ligands, forced to interact with a bromide anion in Figure 2b [22], is here observed to be a prominent docking site for neutral iodine molecules. Contrary to what is observed with simpler protonated amines [11], where an active dialogue is established between halogen and hydrogen bonding, here the interactions between the charged ligands and iodine-based species mainly involves the external hydrophobic surface of the azacyclophane, bringing its shape into the spotlight.

Perhaps the most prominent crystal engineering piece of information that we can derive from the present study is the possibility to use charged azacyclophanes as templating agents for the synthesis of polyiodides. Despite some of this being reported for linear polyiodides (I_3^-, I_4^{2-}, I_6^{2-}) in the case of aliphatic [11] or aromatic [6] linear ammonium derivatives, in the current case we appear to be in the presence of the first three-dimensional mold reported for the synthesis of the I_7^- anion, moreover a species which can be considered of quite rare occurrence (only 10 structures reported so far in the CSD feature I_7^- [29–38], only half of them containing selectively I_7^- rather than a mixture of different polyiodide species [31–35]). As we tried to portray in Figure 12, the diprotonated H_2L–Me_3 ligand possesses a stunning complementarity with the two interacting heptaiodide anions. No matter the point of view, we are always able to distinguish complementary and stabilizing structural elements, such as the curvature of the ligand with respect to the polyiodide angles (Figure 12a,d), the perfect fitting of the phenolic O in the assembly of the anions (red, Figure 12a–d), the templating role of the methyl substituents (Figure 12b–d) and that of the charged crevice defined by the ammonium groups, perfectly matched by one of the I_7^- axes (blue, Figure 12c). According to the extraordinary complementarity observed, we are led to believe that the selective observation of I_7^- anions in the crystal structure, and of them only, is due to the capacity of the diprotonated form of this ligand to act as a supramolecular templating agent, molding the heptaiodide anion around itself.

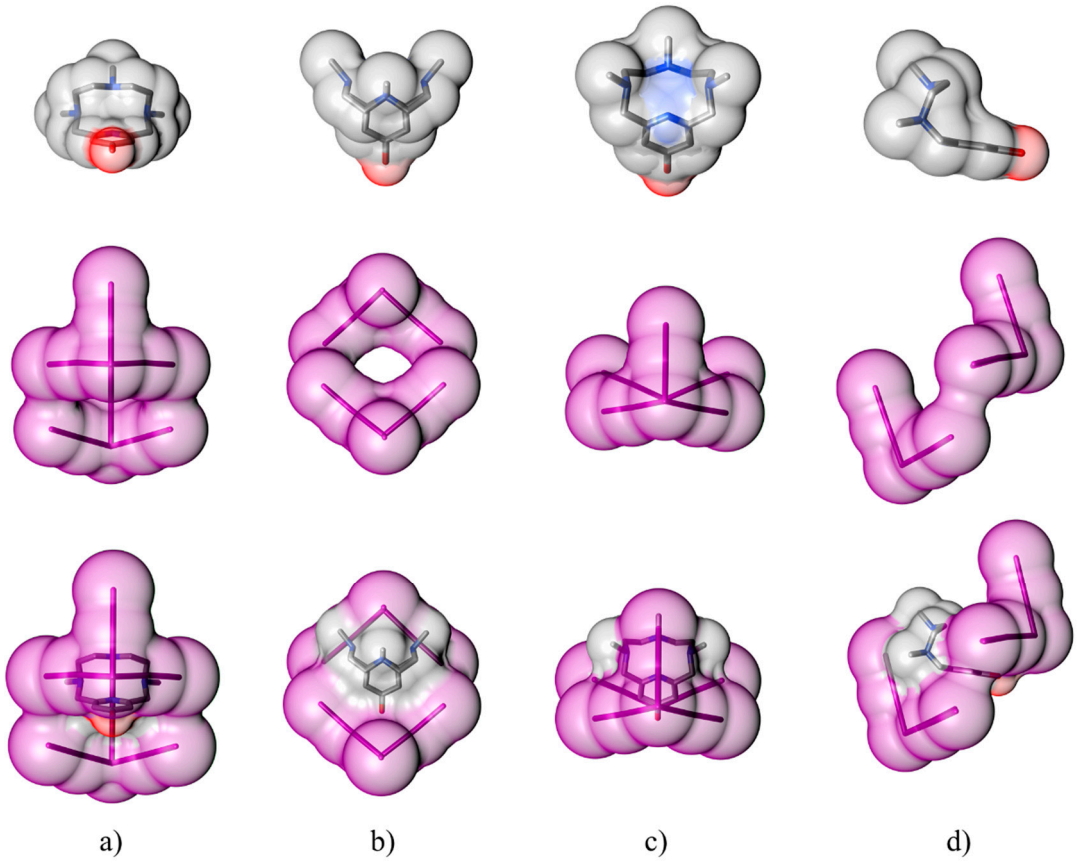

Figure 12. Detailed different views of the $H_2L2–Me_3^{2+}$ ligand (top), of the two closest non-equivalent interacting I_7^- anions (middle) and of their perfectly complementary complex (bottom), suggesting the templating action of the ligand in orchestrating the selective formation of this polyiodide anion over all the possible others. (**a**) front, (**b**) top, (**c**) back and (**d**) side view of the heptaiodide complex. Color code: grey, C; cyan, N; red, O; violet, I.

4. Materials and Methods

4.1. Ligand Synthesis

The synthesis of the compounds 3,6,9-triaza-1(2,6)-pyridinecyclodecaphane (L1·3HBr) [39–42], 6-(*N*-methyl)-3,6,9-triaza-1(2,6)-pyridinacyclodecaphane (L1–Me·3HBr) [42], 3,6,9-tris(*N*-methyl)-3,6,9-triaza-1(2,6)-pyridinacyclodecaphane (L1–Me_3·3HCl) [43–45] (Figure 3) 4-methyl-1,7-bis(*p*-tolylsulfonyl)-1,4,7-triazaheptane (2·3HCl) [23,42] and 4-benzyloxy-2,6-bis(bromomethyl)pyridine (py-obn) [46–48] (Figure 13) were carried out following the procedure described previously in the literature. All reagents were obtained from commercial sources and used as received. Solvents used for the chemical synthesis were of analytical grade and used without further purification. Characterization of the compounds can be found in the Supplementary Materials (Figures S1–S18).

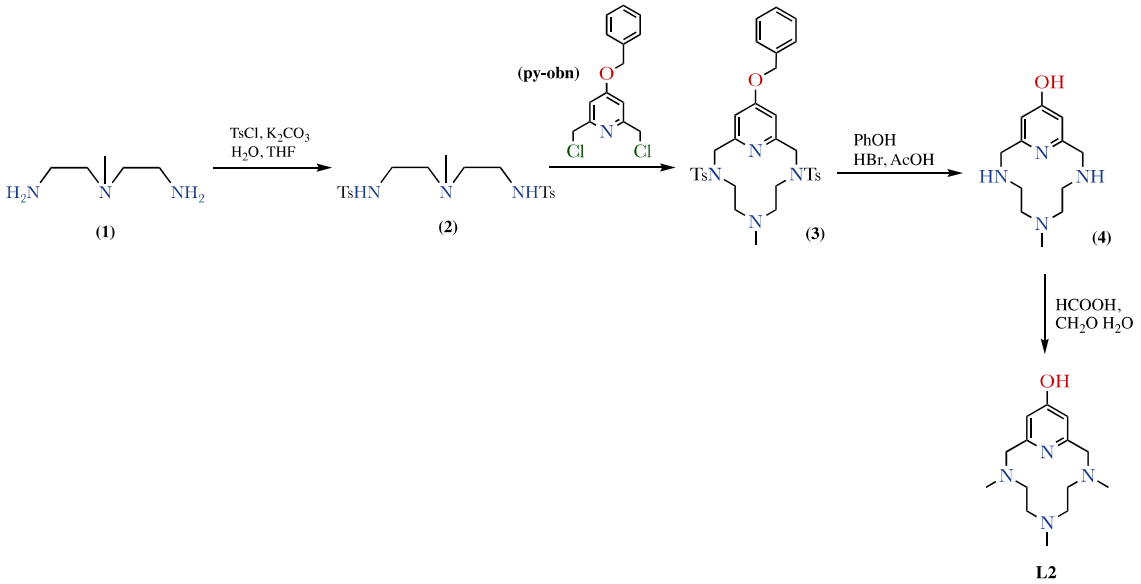

Figure 13. Chemical synthesis of ligand L2–Me_3 from commercially available polyamine **1** and the synthesized pyridine derivative **py-obn**.

4.1.1. Synthesis of 14-Benziloxy-6-(*N*-methyl)-3,9-bis(*p*-tolylsulfonyl)-3,6,9-triaza-1(2,6)-pyridinacyclodecaphane (**3**)

The procedure used was adapted from references [49–51].

4-Methyl-1,7-bis(p-tolylsulfonyl)-1,4,7-triazaheptane (**2**, 2.20 g, 5.16 mmol) and K_2CO_3 (4.29 g, 31.00 mmol) were suspended in anhydrous CH_3CN (150 cm^3), and the mixture was stirred and heated to reflux. Then, the pyridine derivative **py-obn** (1.60 g, 5.69 mmol) was dissolved in 50 cm^3 of anhydrous CH_3CN and added dropwise over the previous suspension. The mixture was left at reflux under N_2 inert atmosphere for 24 h. Once the reaction time had elapsed, the suspension was cooled down and the carbonate salts were filtered off. The solvent was evaporated under reduced pressure, giving rise to a brown oil. This product was then suspended in ethanol and refluxed for 4 h. During the reflux, a white solid came up, which was filtered and washed with cold EtOH. Product **3** was obtained as a pale yellow solid (1.15 g, 35%). Characterization data of the compound are included in the Supplementary Materials (Figures S4–S6). ^{1}H NMR (300.1 MHz, $CDCl_3$), δ (ppm): 7.72 (d, J = 8.3 Hz, 4H), 7.47–7.35 (m, 5H), 7.32 (d, J = 8.5 Hz, 4H), 6.80 (s, 2H), 5.03 (s, 2H), 4.29 (s, 4H), 3.21–3.06 (m, 4H), 2.41 (s, 6H), 2.39–2.31 (m, 4H), 2.20 (s, 3H). ^{13}C NMR (75.4 MHz, $CDCl_3$), δ (ppm): 167.1, 156.9, 143.9, 136.5, 135.6, 130.2, 129.2, 128.9, 128.1, 127.6, 110.9, 70.6, 54.9, 52.9, 44.4, 43.7, 31.3, 21.9. MS (ESI) m/z: 635.1 g·mol^{-1}, corresponding to $[M + H]^+$.

4.1.2. Synthesis of 6-(*N*-Methyl)-3,6,9-triaza-1(2,6)-pyridinacyclodecaphan-14-ol hydrobromide (**4**·3HBr)

Deprotection was achieved by a modification of the procedure described in reference [52].

3 (0.5 g, 0.79 mmol) and phenol (2.82 g, 30.01 mmol) were suspended in HBr–AcOH 33% (30 cm^3). The mixture was stirred at 90 °C for further 48 h and cooled. The resulting suspension was filtered and washed several times with EtOH anhydrous to give the product **4** in a salt form (0.31 g, 82%). Characterization data of the compound are included in the Supplementary Materials (Figures S7–S9). ^{1}H NMR (300.1 MHz, D_2O), δ (ppm): 6.94 (s, 2H), 4.55–4.46 (m, 4H), 3.35–3.27 (m, 4H), 2.68 (t, J = 5.5 Hz, 4H), 2.46 (s, 3H). ^{13}C NMR (75.4 MHz, D_2O), δ (ppm): 166.5, 151.5, 110.3, 52.9, 50.4, 46.0, 42.0. MS (ESI) m/z: 236.9 g·mol^{-1}, corresponding to $[M + H]^+$

4.1.3. Synthesis of 3,6,9-Tris(*N*-methyl)-3,6,9-triaza-1(2,6)-pyridinacyclodecaphan-14-ol (**L2–Me_3**)

The procedure used was adapted from references [43,44].

4 (0.71 g, 1.48 mmol) was dissolved in Milli-Q water (30 cm^3), formaldehyde 37% (1.23 cm^3, 44.4 mmol), and formic acid (1.70 cm^3, 44.4 mmol), and the resulting mixture was then refluxed for 72 h. After cooling down, the solvent was removed under reduced pressure, obtaining a powder solid (0.97 g, >98%). Characterization data of the compound are included in the Supplementary Materials (Figures S10–S12). ^{1}H NMR (300.1 MHz, D_2O), δ (ppm): 8.23 (s, 1H), 6.96 (s, 2H), 4.62 (s, 4H), 3.53 (t, J = 5.5 Hz, 4H), 3.17 (s, 6H), 2.92–2.71 (m, 4H), 2.56 (s, 3H). ^{13}C NMR (75.4 MHz, D_2O), δ (ppm): 165.6, 150.8, 110.5, 60.5, 55.1, 51.9, 44.4, 41.3. MS (ESI) m/z: 265.1 $g{\cdot}mol^{-1}$, corresponding to $[M + H]^+$. Anal. Calc. for $C_{14}H_{24}ON_4(HCl)_3(H_2O)_2(NaCl)_{3.9}$: C, 26.7; H, 4.9; N, 8.5: Found: C, 26.4; H, 4.9; N, 8.8.

4.2. X-ray Structure Analysis

$[(H_2L1)_2(I_2)(I_5)(I_3)_3]$ and $[H_2L2–Me_3(I_7)_2]$ dark brown crystals have been obtained within several weeks by slow diffusion of acidic aqueous solution of the ligands towards an iodine rich I_2/I^- aqueous mixture (I_2:I^- ratio 2:1) inside an H-shaped tube.

Crystallographic data have been deposited with the Cambridge Crystallographic Data Center, CCDC numbers: CCDC 1900332 ($[(H_2L1)_2I_2(I_5)(I_3)_3]$) and CCDC 1900333 ($[H_2L2–Me_3(I_7)_2]$). These data can be obtained free of charge from the CCDC at www.ccdc.cam.ac.uk.

4.2.1. Crystallographic Information for $[(H_2L1)_2I_2(I_5)(I_3)_3]$

$C_{22}H_{40}I_{16}N_8$ (M = 2447.02 g/mol): triclinic, space group $P-1$ (no. 2), a = 8.300(1) Å, b = 16.191(2) Å, c = 21.221(3) Å, α = 108.167(4)°, β = 94.071(5)°, γ = 104.453(4)°, V = 2589.5(6) $Å^3$, Z = 2, T = 100 K, μ(Mo Kα) = 9.586 mm^{-1}, Dcalc = 3.138 g/cm^3, 59174 reflections measured (2.543° ≤ Θ ≤ 25.350°), 9410 unique (Rint = 0.0619, Rsigma = 0.0404) which were used in all calculations. Absorption correction was performed by SADABS-2016/2 [53]. Structure solved by direct methods (*SHELXLS*) [54]. Refinements attained by means of full-matrix least-squares using *SHELXL* Version 2014/7 [55]. The final $R1$ was 0.0377 ($I > 2\sigma(I)$) and $wR2$ was 0.1083 (all data).

4.2.2. Crystallographic Information for $[H_2L2–Me_3(I_7)_2]$

$C_{14}H_{23}I_{14}N_4O$ (M = 2039.96 g/mol): monoclinic, space group $P2_1/m$ (no. 11), a = 9.226(1) Å, b = 13.060(1) Å, c = 17.377(2) Å, β = 104.671(3)°, V = 2025.5(4) $Å^3$, Z = 2, T = 100 K, μ(Mo Kα) = 10.714 mm^{-1}, Dcalc = 3.345 g/cm^3, 3116 reflections measured (2.282° ≤ Θ ≤ 25.022°), 2810 unique (Rint = 0.0469, Rsigma = 0.0848) which were used in all calculations. Absorption correction was performed by SADABS-2016/2 [53] Structure was solved by direct methods (*SHELXLS*) [54] Refinements attained by means of full-matrix least-squares using *SHELXL* Version 2014/7 [55]. Crystals were twinned with equal component (twin law −1 0 0, 0 −1 0, 0.954 0 1). The final $R1$ was 0.0779 ($I > 2\sigma(I)$) and $wR2$ was 0.2353 (all data).

4.2.3. Software

CCDC Mercury [56] and UCSF Chimera [57] programs were used for analysis and graphical presentation of data.

5. Conclusions

Halogen bonding [58–65], incorporation of iodine molecules within three-dimensional networks [66–68] and template synthesis of specific polyiodides [4–6,9,10] are current topics in polyiodide chemistry. We contribute to the discussion with the proposition of small protonated azacyclophanes as a meaningful class of stabilizing ligands capable of producing high-density iodine packings, of which we discuss two examples. I_N is proposed as a simple quantitative parameter to compare the macroscopic density of iodine packing among different crystal structures. Moreover, diprotonated form of the L2–Me_3 ligand is suggested as the first templating agent capable of promoting selectively the formation of the I_7^- anion. We can safely anticipate the crystal engineering directed

assembly of iodine-based clathrate-like compounds to produce technologically relevant materials in the near future.

Supplementary Materials: The following are available online at http://www.mdpi.com/2304-6740/7/4/48/s1: Table S1: Hydrogen bonds found in the $[(H_2L1)_2I_2(I_5)(I_3)_3]$ crystal structure; Figures S1–S18: 1H-NMR, 13C-NMR and MS spectra of synthesized derivatives; CIF and checkCIF files.

Author Contributions: Conceptualization, M.S., E.G.-E. and A.B.; methodology, all authors; validation, P.M.; formal analysis, C.B.; investigation, M.S., Á.M.-C.; resources, Á.M.-C., B.V., E.D.-P.; writing—original draft preparation, M.S.; writing—review and editing, all authors.; visualization, M.S., Á.M.-C., C.B.; supervision, J.M.L., E.G.-E. and A.B.; project administration, E.G.-E. and A.B.; funding acquisition, E.G.-E. and A.B.

Funding: This research was funded by the Spanish Ministry of Economy and Business, grant number CTQ2017-90852-REDC, the Spanish Ministry of Science, Innovation and Universities, grants number FPU14/05098 and EST17/00666, and the Italian MIUR (project 2015MP34H3).

Conflicts of Interest: The authors declare no conflict of interest.

References

1. Gay-Lussac, J.L. Mémoire sur l'iode. *Ann. Chimie* **1814**, *91*, 5–160.
2. Jones, G. On the Existence and Behavior of Complex Polyiodides. *J. Phys. Chem.* **1930**, *34*, 673–691. [CrossRef]
3. Svensson, P.H.; Kloo, L. Synthesis, structure, and bonding in polyiodide and metal iodide-iodine systems. *Chem. Rev.* **2003**, *103*, 1649–1684. [CrossRef] [PubMed]
4. Svensson, P.H.; Gorlov, M.; Kloo, L. Dimensional caging of polyiodides. *Inorg. Chem.* **2008**, *47*, 11464–11466. [CrossRef] [PubMed]
5. Abate, A.; Brischetto, M.; Cavallo, G.; Lahtinen, M.; Metrangolo, P.; Pilati, T.; Radice, S.; Resnati, G.; Rissanen, K.; Terraneo, G. Dimensional encapsulation of $I^-\cdots I_2\cdots I^-$ in an organic salt crystal matrix. *Chem. Commun.* **2010**, *46*, 2724–2726. [CrossRef] [PubMed]
6. García, M.D.; Martí-Rujas, J.; Metrangolo, P.; Peinador, C.; Pilati, T.; Resnati, G.; Terraneo, G.; Ursini, M. Dimensional caging of polyiodides: Cation-templated synthesis using bipyridinium salts. *CrystEngComm* **2011**, *13*, 4411–4416. [CrossRef]
7. Reiss, G.J.; van Megen, M. Two new polyiodides in the 4,4′-bipyridinium diiodide/iodine system. *Z. Nat. B* **2012**, *67*, 5–10.
8. Van Megen, M.; Reiss, G.J. The pseudosymmetric structure of bis(pentane-1,5-diaminium) iodide tris(triiodide). *Acta Cryst. E* **2012**, *68*, o1331–o1332. [CrossRef]
9. Garzón-Tovar, L.; Duarte-Ruiz, Á.; Wurst, K. Non-classical hydrogen bond (CH···I) directed self-assembly formation of a novel 1D supramolecular polymer, based on a copper complex $[Cu\{(CH_3)_2SO\}_6]I_4$. *Inorg. Chem. Commun.* **2013**, *32*, 64–67. [CrossRef]
10. Müller, M.; Albrecht, M.; Gossen, V.; Peters, T.; Hoffmann, A.; Raabe, G.; Valkonen, A.; Rissanen, K. Anion–π interactions in salts with polyhalide anions: Trapping of I_4^{2-}. *Chem. Eur. J.* **2010**, *16*, 12446–12453. [CrossRef]
11. Van Megen, M.; Reiss, G.J. I_6^{2-} Anion Composed of Two Asymmetric Triiodide Moieties: A Competition between Halogen and Hydrogen Bond. *Inorganics* **2013**, *1*, 3–13. [CrossRef]
12. Wu, J.; Lan, Z.; Lin, J.; Huang, M.; Huang, Y.; Fan, L.; Luo, G. Electrolytes in Dye-Sensitized Solar Cells. *Chem. Rev.* **2015**, *115*, 2136–2173. [CrossRef] [PubMed]
13. Bella, F.; Galliano, S.; Falco, M.; Viscardi, G.; Barolo, C.; Gratzel, M.; Gerbaldi, C. Unveiling iodine-based electrolytes chemistry in aqueous dye-sensitized solar cells. *Chem. Sci.* **2016**, *7*, 4880–4890. [CrossRef]
14. De Grotthus, C.J.D. Sur la décomposition de l'eau et des corps qu'elle tient en dissolution à l'aide de l'électricité galvanique. *Ann. Chim.* **1806**, *58*, 54–73.
15. Li, J.; Wang, Z.-S. Lithium-coordinating ionic conductor for solid-state dye-sensitized solar cells. *RSC Adv.* **2015**, *5*, 56967–56973. [CrossRef]
16. Wang, H.; Li, J.; Gong, F.; Zhou, G.; Wang, Z.-S. Ionic Conductor with High Conductivity as Single-Component Electrolyte for Efficient Solid-State Dye-Sensitized Solar Cells. *J. Am. Chem. Soc.* **2013**, *135*, 12627–12633. [CrossRef] [PubMed]
17. Wang, H.; Li, H.; Xue, B.; Wang, Z.; Meng, Q.; Chen, L. Solid-State Composite Electrolyte LiI/3-Hydroxypropionitrile/SiO_2 for Dye-Sensitized Solar Cells. *J. Am. Chem. Soc.* **2005**, *127*, 6394–6401. [CrossRef]

18. Savastano, M.; Bazzicalupi, C.; Giorgi, C.; García-Gallarín, C.; López de la Torre, M.D.; Pichierri, F.; Bianchi, A.; Melguizo, M. Anion Complexes with Tetrazine-Based Ligands: Formation of Strong Anion–π Interactions in Solution and in the Solid State. *Inorg. Chem.* **2016**, *55*, 8013–8024. [CrossRef]
19. Savastano, M.; Bazzicalupi, C.; García-Gallarín, C.; Gellini, C.; López de la Torre, M.D.; Mariani, P.; Pichierri, F.; Bianchi, A.; Melguizo, M. Iodide and triiodide anion complexes involving anion–π interactions with a tetrazine-based receptor. *Dalton Trans.* **2017**, *46*, 4518–4529. [CrossRef] [PubMed]
20. Bianchi, A.; García-España, E. Azacoronands and Azacyclophanes. In *Supramolecular Chemistry: From Molecules to Nanomaterials*; Gale, P.A., Steed, J.W., Eds.; John Wiley & Sons, Ltd.: Hoboken, NJ, USA, 2012. [CrossRef]
21. Ilioudis, C.A.; Steed, J.W. Complexation of I_4^{2-} and I_8^{2-} by protonated azacyclophanes. *CrystEngComm* **2004**, *6*, 239–242. [CrossRef]
22. Drahos, B.; Kotek, J.; Cisarova, I.; Hermann, P.; Helm, L.; Lukes, I.; Toth, E. Mn^{2+} Complexes with 12-Membered Pyridine Based Macrocycles Bearing Carboxylate or Phosphonate Pendant Arm: Crystallographic, Thermodynamic, Kinetic, Redox, and $^{1}H/^{17}O$ Relaxation Studies. *Inorg. Chem.* **2011**, *50*, 12785–12801. [CrossRef] [PubMed]
23. Martínez-Camarena, Á.; Liberato, A.; Delgado-Pinar, E.; Algarra, A.G.; Pitarch-Jarque, J.; Llinares, J.M.; Mañez, M.Á.; Domenech-Carbó, A.; Basallote, M.G.; García-España, E. Coordination Chemistry of Cu^{2+} Complexes of Small *N*-Alkylated Tetra-azacyclophanes with SOD Activity. *Inorg. Chem.* **2018**, *57*, 10961–10973. [CrossRef] [PubMed]
24. Verdejo, B.; Ferrer, A.; Blasco, S.; Castillo, C.E.; Gonzalez, J.; Ĺatorre, J.; Máñez, M.A.; Basallote, M.G.; Soriano, C.; García España, E. Hydrogen and Copper Ion-Induced Molecular Reorganizations in Scorpionand-like Ligands. A Potentiometric, Mechanistic, and Solid-State Study. *Inorg. Chem.* **2007**, *46*, 5707–5719. [CrossRef] [PubMed]
25. Alcock, N.W. Secondary Bonding to Nonmetallic Elements. *Adv. Inorg. Chem. Radiochem.* **1972**, *15*, 1–58. [CrossRef]
26. Savastano, M.; Arranz-Mascarós, P.; Bazzicalupi, C.; Clares, M.P.; Godino-Salido, M.L.; Gutiérrez-Valero, M.D.; Inclán, M.; Bianchi, A.; García-España, E.; López-Garzón, R. Construction of green nanostructured heterogeneous catalysts via non-covalent surface decoration of multi-walled carbon nanotubes with Pd(II) complexes of azamacrocycles. *J. Catal.* **2017**, *353*, 239–249. [CrossRef]
27. Bazzicalupi, C.; Bencini, A.; Biagini, S.; Bianchi, A.; Faggi, E.; Giorgi, C.; Marchetta, M.; Totti, F.; Valtancoli, B. Polyamine receptors containing dipyridine or phenanthroline units: Clues for the design of fluorescent chemosensors for metal ions. *Chem. Eur. J.* **2009**, *15*, 8049–8063. [CrossRef] [PubMed]
28. Alvarez, S. A cartography of the van der Waals territories. *Dalton Trans.* **2013**, *42*, 8617–8636. [CrossRef] [PubMed]
29. Rimmer, E.L.; Bailey, R.D.; Pennington, W.T.; Hanks, T.W. The reaction of iodine with 9-methylacridine: Formation of polyiodide salts and a charge-transfer complex. *J. Chem. Soc. Perkin Trans. 2* **1998**, 2557–2562. [CrossRef]
30. Aragoni, M.C.; Arca, M.; Demartin, F.; Devillanova, F.A.; Garau, A.; Isaia, F.; Lippolis, V.; Rizzato, S.; Verani, G. $[Ni(L)(MeCN)]^{2+}$ complex cation as a template for the assembly of extended $I_3^-\cdots I_5^-$ and $I_5^-\cdots I_7^-$ polyiodide networks {L = 2,5,8-trithia[9](2,9)-1,10-phenanthrolinophane}. Synthesis and structures of $[Ni(L)(MeCN)]I_8$ and $[Ni(L)(MeCN)]I_{12}$. *Inorg. Chim. Acta* **2004**, *357*, 3803–3809. [CrossRef]
31. Demartin, F.; Deplano, P.; Devillanova, F.A.; Isaia, F.; Lippolis, V.; Verani, G. Conductivity, FT-Raman spectra, and X-ray crystal structures of two novel $[D_2I]I_n$ (n = 3 and D = *N*-methylbenzothiazole-2(3*H*)-selone; n = 7 and D = *N*-methylbenzothiazole-2(3*H*)-thione) iodonium salts. First example of I−·3I2 heptaiodide. *Inorg. Chem.* **1993**, *32*, 3694–3699. [CrossRef]
32. Corban, G.J.; Hadjikakou, S.K.; Tsipis, A.C.; Kubicki, M.; Bakas, T.; Hadjiliadis, N. Inhibition of peroxidase-catalyzed iodination by thioamides: Experimental and theoretical study of the antithyroid activity of thioamides. *New J. Chem.* **2011**, *35*, 213–224. [CrossRef]
33. Tebbe, K.; Nagel, K. Untersuchungen an Polyhalogeniden. XXVI [1]. Über *N*-Propylurotropiniumpolyiodide UrPrIx mit x = 5 und 7: Strukturelle Charakterisierung eines Pentaiodids und eines Heptaiodids. *Zeitschrift Anorganische Allgemeine Chemie* **1996**, *622*, 1323–1328. [CrossRef]
34. Poli, R.; Gordon, J.C.; Khanna, R.K.; Fanwick, P.E. The first discrete structure for the heptaiodide ion. *Inorg. Chem.* **1992**, *31*, 3165–3167. [CrossRef]

35. Renner, M.W.; Barkigia, K.M.; Zhang, Y.; Medforth, C.J.; Smith, K.M.; Fajer, J. Consequences of Oxidation in Nonplanar Porphyrins: Molecular Structure and Diamagnetism of the. pi. Cation Radical of Copper(II) Octaethyltetraphenylporphyrin. *J. Am. Chem. Soc.* **1994**, *116*, 8582–8592. [CrossRef]
36. Svensson, P.H.; Raud, G.; Kloo, L. Metal Iodides in Polyiodide Networks—The Structural Chemistry of Complex Thallium Iodides with Excess Iodine. *Eur. J. Inorg. Chem.* **2000**, 1275–1282. [CrossRef]
37. Fiolka, C.; Pantenburg, I.; Meyer, G. Transition-Metal(II)–Crown-Ether–Polyiodides. *Cryst. Growth Des.* **2011**, *11*, 5159–5165. [CrossRef]
38. Hendrixson, T.L.; ter Horst, M.A.; Jacobson, R.A. Structure of dipyridinium decaiodide—An infinite chain structure. *Acta Cryst.* **1991**, *C47*, 2141–2144. [CrossRef]
39. Stetter, H.; Frank, W.; Mertens, R. Darstellung und komplexbildung von polyazacycloalkan-*N*-essigsäuren. *Tetrahedron* **1981**, *37*, 767–772. [CrossRef]
40. Wu, C.; He, Y. Synthesis of azacrown containing pyridine ring. *Youji Huaxue* **1983**, *3*(6), 437–439.
41. Costa, J.; Delgado, R. Metal complexes of macrocyclic ligands containing pyridine. *Inorg. Chem.* **1993**, *32*, 5257–5265. [CrossRef]
42. Meijer, A. Manganese chelates and their use as contrast agents in magnetic resonance imaging (MRI). U.S. Patent WO 2011/073371 A1, 23 June 2011.
43. Eschweile, W. Ersatz von an Stickstoff gebundenen Wasserstoffatomen durch die Methylgruppe mit Hülfe von Formaldehyd. *Berichte Deutschen Chemischen Gesellschaft* **1905**, *38*, 880–882. [CrossRef]
44. Clarke, H.T.; Gillespie, B.H.; Weisshaus, S.Z. The Action of Formaldehyde on Amines and Amino Acids. *J. Am. Chem. Soc.* **1933**, *55*, 4571–4587. [CrossRef]
45. Serrano-Plana, J.; Oloo, W.N.; Acosta-Rueda, L.; Meier, K.K.; Verdejo, B.; García-España, E.; Basallote, M.G.; Münck, E.; Que, L.; Company, A.; et al. Trapping a Highly Reactive Nonheme Iron Intermediate That Oxygenates Strong C–H Bonds with Stereoretention. *J. Am. Chem. Soc.* **2015**, *137*, 15833–15842. [CrossRef]
46. Busto, E.; González-Álvarez, A.; Gotor-Fernández, V.; Alfonso, I.; Gotor, V. Optically active macrocyclic hexaazapyridinophanes decorated at the periphery: Synthesis and applications in the NMR enantiodiscrimination of carboxylic acids. *Tetrahedron* **2010**, *66*, 6070–6077. [CrossRef]
47. Froidevaux, P.; Harrowfield, J.M.; Sobolev, A.N. Calixarenes as Scaffolds: Introduction of Tridentate Rare Earth Metal Binding Units into Calix[4]arene. *Inorg. Chem.* **2000**, *39*, 4678–4687. [CrossRef] [PubMed]
48. Martínez-Camarena, Á.; Delgado-Pinar, E.; Soriano, C.; Alarcón, J.; Llinares, J.M.; Tejero, R.; García-España, E. Enhancement of SOD activity in boehmite supported nanoreceptors. *Chem. Commun.* **2018**, *54*, 3871–3874. [CrossRef]
49. Richman, J.E.; Atkins, T.J. Nitrogen analogs of crown ethers. *J. Am. Chem. Soc.* **1974**, *96*, 2268–2270. [CrossRef]
50. Richman, J.E.; Atkins, T.J.; Oetle, W.T. *Organic Synthesis*; John Wiley & Sons, Inc.: Hoboken, NJ, USA, 1988; Volume VI.
51. Shaw, B.L. Formation of large rings, internal metalation reactions, and internal entropy effects. *J. Am. Chem. Soc.* **1975**, *97*, 3856–3857. [CrossRef]
52. Haskell, B.E.; Bowlus, S.B. New synthesis of L-2-amino-3-oxalylaminopropionic acid, the Lathyrus sativus neurotoxin. *J. Org. Chem.* **1976**, *41*, 159–160. [CrossRef]
53. Krause, L.; Herbst-Irmer, R.; Sheldrick, G.M.; Stalke, D. Comparison of silver and molybdenum microfocus X-ray sources for single-crystal structure determination. *J. Appl. Cryst.* **2015**, *48*, 3–10. [CrossRef]
54. Sheldrick, G.M. A short history of *SHELX*. *Acta Cryst.* **2008**, *A64*, 112–122. [CrossRef]
55. Sheldrick, G.M. Crystal structure refinement with *SHELXL*. *Acta Cryst.* **2015**, *C71*, 3–8. [CrossRef]
56. Macrae, C.F.; Bruno, I.J.; Chisholm, J.A.; Edgington, P.R.; McCabe, P.; Pidcock, E.; Rodriguez-Monge, L.; Taylor, R.; van de Streek, J.; Wood, P.A. Mercury CSD 2.0—New features for the visualization and investigation of crystal structures. *J. Appl. Cryst.* **2008**, *41*, 466–470. [CrossRef]
57. Pettersen, E.F.; Goddard, T.D.; Huang, C.C.; Couch, G.S.; Greenblatt, D.M.; Meng, E.C.; Ferrin, T.E. UCSF Chimera—A visualization system for exploratory research and analysis. *J. Comput. Chem.* **2004**, *25*, 1605–1612. [CrossRef] [PubMed]
58. Cavallo, G.; Murray, J.S.; Politzer, P.; Pilati, T.; Ursini, M.; Resnati, G. Halogen bonding in hypervalent iodine and bromine derivatives: Halonium salts. *IUCrJ* **2017**, *4 (Pt 4)*, 411–419. [CrossRef]
59. Catalano, L.; Cavallo, G.; Metrangolo, P.; Resnati, G.; Terraneo, G. Halogen Bonding in Hypervalent Iodine Compounds. In *Hypervalent Iodine Chemistry*; Wirth, T., Ed.; Topics in Current Chemistry; Springer: Cham, Switzerland, 2016; Volume 373.

60. Terraneo, G.; Resnati, G.; Metrangolo, P. Iodine and Halogen Bonding. In *Iodine Chemistry and Applications*; Kaiho, T., Ed.; John Wiley & Sons, Inc.: Hoboken, NJ, USA, 2015.
61. Bartashevich, E.V.; Yushina, I.D.; Stash, A.I.; Tsirelson, V.G. Halogen Bonding and Other Iodine Interactions in Crystals of Dihydrothiazolo(oxazino)quinolinium Oligoiodides from the Electron-Density Viewpoint. *Cryst. Growth Des.* **2014**, *14*, 5674–5684. [CrossRef]
62. Arman, H.D.; Gieseking, R.L.; Hanks, T.W.; Pennington, W.T. Complementary halogen and hydrogen bonding: Sulfur···iodine interactions and thioamide ribbons. *Chem. Commun.* **2010**, *46*, 1854–1856. [CrossRef] [PubMed]
63. Arman, H.D.; Rafferty, E.R.; Bayse, C.A.; Pennington, W.T. Complementary Selenium···Iodine Halogen Bonding and Phenyl Embraces: Cocrystals of Triphenylphosphine Selenide with Organoiodides. *Cryst. Growth Des.* **2012**, *12*, 4315–4323. [CrossRef]
64. Bartashevich, E.; Yushina, I.; Kropotina, K.; Muhitdinova, S.; Tsirelson, V. Testing the tools for revealing and characterizing the iodine–iodine halogen bond in crystals. *Acta Cryst. B* **2017**, *73*, 217–226. [CrossRef] [PubMed]
65. Resnati, G.; Pennington, W.T. The halogen bond: A new avenue in recognition and self-assembly. *New J. Chem.* **2018**, *42*, 10461–10462. [CrossRef]
66. Peuronen, A.; Valkonen, A.; Kortelainen, M.; Rissanen, K.; Lahtinen, M. Halogen bonding-based "catch and release": Reversible solid-state entrapment of elemental iodine with monoalkylated dabco salts. *Cryst. Growth Des.* **2012**, *12*, 4157–4169. [CrossRef]
67. Hu, J.; Wang, D.; Guo, W.; Du, S.; Tang, Z.K. Reversible control of the orientation of iodine molecules inside the AlPO4–11 crystals. *J. Phys. Chem. C* **2012**, *116*, 4423–4430. [CrossRef]
68. Zeng, M.-H.; Wang, Q.-X.; Tan, Y.-X.; Hu, S.; Zhao, H.-X.; Long, L.-S.; Kurmoo, M. Rigid pillars and double walls in a porous metal-organic framework: Single-crystal to single-crystal, controlled uptake and release of iodine and electrical conductivity. *J. Am. Chem. Soc.* **2010**, *132*, 2561–2563. [CrossRef] [PubMed]